1-1-2020

Exploration of the Dehydrogenation Pathways of Ammonia Diborane and Diammoniate of Diborane by Molecular Dynamics Simulations Using Reactive Force Fields

Peng Gao
University of Wollongong, pg177@uowmail.edu.au

Zhenguo Huang

Haibo Yu
University of Wollongong, hyu@uow.edu.au

Exploration of the Dehydrogenation Pathways of Ammonia Diborane and Diammoniate of Diborane by Molecular Dynamics Simulations Using Reactive Force Fields

Abstract

Ammonium aminodiboranate (AADB) and diammoniate of diborane (DADB) are two isomers of ammonia borane (AB), which have been intensively studied for hydrogen storage. Their high hydrogen contents give them the high potential to serve as hydrogen storage materials. To explore their dehydrogenation pathways, molecular dynamics (MD) simulations with a reactive force field (ReaxFF) were applied. Temperature ramping simulations of their thermolysis were carried out. For AADB, at low temperatures, its hydrogen release can be realized mainly via inter-molecular dehydrogenations. As the temperature of the simulated system increases, the formations of B-N bonds begin to occur. In the case of DADB, we found that this molecule could release hydrogen at a lower temperature with the cleavage of B-N bond. The compositional analysis of the simulated systems was also conducted to monitor the potential intermediates along their dehydrogenation pathways. Our current work provides a detailed picture of the initial dehydrogenation steps of AADB and DADB, and highlights the difference in their respective dehydrogenation processes.

Keywords

force, molecular, diammoniate, dynamics, simulations, fields, reactive, diborane, exploration, pathways, dehydrogenation, ammonia

Publication Details

Gao, P., Huang, Z. & Yu, H. (2020). Exploration of the Dehydrogenation Pathways of Ammonia Diborane and Diammoniate of Diborane by Molecular Dynamics Simulations Using Reactive Force Fields. The Journal of Physical Chemistry A: Isolated Molecules, Clusters, Radicals, and Ions; Environmental Chemistry, Geochemistry, and Astrochemistry; Theory, Online First 1-20.

Exploration of the Dehydrogenation Pathways of Ammonia Diborane and Diammoniate of Diborane by Molecular Dynamics Simulations Using Reactive Force Fields

Peng Gao,[†,‡] Zhenguo Huang,[¶] and Haibo Yu[*,†,‡,§]

†*School of Chemistry and Molecular Bioscience, University of Wollongong, NSW 2500, Australia*

‡*Molecular Horizons, University of Wollongong, NSW 2500, Australia*

¶*School of Civil and Environmental Engineering, University of Technology Sydney, NSW 2007, Australia*

§*Illawarra Health and Medical Research Institute, Wollongong, Australia*

E-mail: hyu@uow.edu.au

Phone: +61 (2) 4221 4235. Fax: +61 (2) 4221 4287

Abstract

Ammonium aminodiboranate (AADB) and diammoniate of diborane (DADB) are two isomers of ammonia borane (AB), which have been intensively studied for hydrogen storage. Their high hydrogen contents give them the high potential to serve as hydrogen storage materials. To explore their dehydrogenation pathways, molecular dynamics (MD) simulations with a reactive force field (ReaxFF) were applied. Temperature ramping simulations of their thermolysis were carried out. For AADB, at low temperatures, its hydrogen release can be realized mainly via inter-molecular dehydrogenations. As the temperature of the simulated system increases, the formations of B–N bonds begin to occur. In the case of DADB, we found that this molecule could release hydrogen at a lower temperature with the cleavage of B–N bond. The compositional analysis of the simulated systems was also conducted to monitor the potential intermediates along their dehydrogenation pathways. Our current work provides a detailed picture of the initial dehydrogenation steps of AADB and DADB, and highlights the difference in their respective dehydrogenation processes.

Introduction

Hydrogen has been widely regarded as an ideal energy source due to its environmental friendliness and its high combustion energy per mass unit.[1] However, the largest challenge for the widespread applications of hydrogen lies in its storage and delivery, which has traditionally relied on compression and liquefaction that cause significant energy penalty.[2] Therefore, the successful development of efficient and safe storage media is crucial.[2,3] Materials-based hydrogen storage has emerged as a potential solution, including metal hydrides,[4–7] liquid hydrocarbons,[8] and newly emerging nitrogen and boron-containing compounds.[9–12]

In recent years, the studies of ammonia borane (AB, NH_3-BH_3) have drawn considerable attention.[13–16] In addition to its high hydrogen content, its thermolysis has mild operating conditions in terms of temperature and pressure. Moreover, through the con-

trol of reaction conditions or applications of catalysis, its dehydrogenation can be further enhanced.[17–19] Both experimental and computational studies revealed that there are two important isomers of AB: ammonium aminodiboranate (AADB, composed of $[NH_4]^+$ and $[BH_3-NH_2-BH_3]^-$)[20–24] and diammoniate of diborane (DADB, composed of $[BH_4]^-$ and $[NH_3-BH_2-NH_3]^+$).[24–26] The detailed reaction pathways and energy landscapes for the dehydrogenation of AB have been studied by high-level electronic structure calculations[24] and *ab initio* metadynamics simulations.[23] However, for AADB and DADB, their dehydrogenation mechanisms remain to be investigated. Previously, it has been proposed that DADB will convert to AB and $[NH_2-BH_2]_n$, while AADB to $[NH_2-BH_2-NH_2-BH_2]$ upon heating.[3,24] It has been highlighted that the composition of their nitrogen or boron-containing cation and anion can impact their distinct dehydrogenation pathways.[15,27,28]

To explore the potential of this class of molecules as hydrogen storage materials, an atomistic understanding of the roles played by their B–N bond based skeletons, and the chemical interactions between cations and anions during the dehydrogenation process, is required. However, until now, limited computational studies of these two molecules had been reported.[22,27] This is largely due to the complexity of their intra-molecular bonding environment, interactions between cations and anions, as well as the high computational cost of such studies with *ab initio* or density functional theory (DFT) methods. Molecular dynamics (MD) simulation with a reactive force field (ReaxFF), which can model chemical reactions but requires much lower computational cost, is a computationally attractive alternative.[29–32] ReaxFF applies the bond orders to model chemical bonding; therefore, breaking and formation of bonds can be simulated. And in recent years, ReaxFF has been applied to the studies of hydrogen storage materials, including BN hydrides,[33,34] boron nitride nanotubes,[35,36] and magnesium hydrides.[37] In this study, we run MD simulations with the ReaxFF developed by Weismiller *et al.*[33] Based on the findings of MD simulations, DFT calculations were further carried out to study their potential dehydrogenation pathways. The stabilities, reaction rates, and dehydrogenation pathways for these two molecules were revealed.

Computational details

Reactive force field (ReaxFF)

To investigate the thermal-stabilities and dehydrogenation pathways of AADB and DADB, MD simulations with the ReaxFF, developed by Weismiller *et al.*,[33] were performed. The key QM data for their parameterization included 1) all the bond dissociation for B/N/O/H combinations; 2) the angular distortions in AB-related molecules; 3) reaction barriers for key reaction steps (H_2 release from AB, dimerization of H_2B-NH_2) and reaction energies associated with H_2 release from AB and with AB oxidation. These key properties cover most of the potential chemistry events envisioned in the dehydrogenation of AADB and DADB. We expect a decent transferability for the ReaxFF parameters by Weismiller *et al.*[33] to study the initial dehydrogenation pathways of AADB and DADB.

Molecular dynamics simulations

A system of 20 molecules randomly placed inside a periodic cubic box with a side length of 3.5 nm was studied. Two different kinds of simulations were performed: temperature ramping simulations and the canonical ensemble simulations (see more details in Table 1). All of the simulations were performed with the package LAMMPS.[38] The time step was set to 0.1 fs. The temperature of the simulated systems was controlled by applying a Nose-Hoover thermostat with the damping constant of 0.1 ps. The trajectories were saved every 1000 steps for further analyses.

Temperature ramping simulations: Experimentally, the dehydrogenations of liquid carbon, boron and nitrogen containing compounds usually take place on a timescale of minutes,[39] which cannot be realised with bruce force simulations on the current computational resources. Instead, the simulation temperatures were increased at a constant heating rate 0.005 K/fs, similar to the work of Weismiller *et al.*[33] For AADB, the system was heated from 500K to 6000K over 1100 ps. For DADB, the system was heated from 200K to 4000K over

760ps. The heating rates and the final temperatures were set to relatively high to achieve nearly complete dehydrogenation within a relatively short simulation time scale (within around one ns).

The canonical ensemble simulations: Furthermore, the temperature-dependent dehydrogenation pathways were studied by carrying out the canonical ensemble simulations for 100 ps (5 repeats) at 1500 K, 2000 K, 2500 K and 3000 K, respectively.

Table 1: Summary of the simulated systems[a]

Simulations	Temperature [K]	Heating rate [K/fs]	Simulation time [ps]
AADB temp. ramping	500–6000	0.005	1100
DADB temp. ramping	200–4000	0.005	760
AADB NVT	1500, 2000, 2500, 3000	N/A	100
DADB NVT	1500, 2000, 2500, 3000	N/A	100

Compositional analysis

The compositional analysis of the simulated trajectories was done through a self-developed script, which uses empirical bonding lengths as the criterion for molecular assignments. Furthermore, for distinguishing the isomers, connectivity between all the atoms assigned within the same molecule will be mapped. A more detailed overview is provided in ESI. The dehydrogenation pathways and the identity of the intermediates were summarized in Table 2. The chemical formulas for these species can be found in ESI Table S1.

Density functional theory calculations

DFT calculations were applied to study the activation barriers in the selected reaction pathways identified in the ReaxFF simulations. All the QM calculations were carried out with Gaussian 09,[40] and M062X/6-311++G(d,p) was adopted following our previous work involving the dehydrogenation of AADB molecules.[22] The transition state structures were verified by normal mode analysis.

Results and Discussions

Temperature ramping MD simulations of AADB and DADB

We characterise the potential dehydrogenation pathways in the temperature ramping simulations by studying the number of released H_2, the rate of hydrogen release per change in temperature, the average molecular weight of the boron and nitrogen containing compounds, and the total number of B–N bonds Figure 1 shows the rates of hydrogen release with the increase of temperature for the simulations of 20 AADB and 20 DADB, respectively (temperature range for AADB: 500K to 6000K, DADB: 200K to 4000K). For AADB, starting from 500K, as the temperature increases, the first hydrogen release occurs at around 800K, and the rate of hydrogen release first peaks at around 1200 K and then decreases; and between 2000K and 2800K, the rate remains nearly constant. And after 2800K, the rate begins to decrease again and then remains substantial until 4500K, where the hydrogen release almost completed. At the end of the simulations, there are four equivalent hydrogen molecules per AADB. The first and second releases occur at around 1500K and 2000K, and the third and fourth hydrogen releases occur at around 3000K and 4000K. Both inter-molecular and intra-molecular dehydrogenations can be observed. The former operates mainly via the reaction between $[NH_4]^+$ and $[BH_3-NH_2-BH_3]^-$, while the latter indicates the dehydrogenation via the dihydrogen interaction between $B-H^{\delta-}$ and $N-H^{\delta+}$ inside the anion $[BH_3-NH_2-BH_3]^-$.

For DADB, we can observe that the first hydrogen release takes place at a much lower temperature, around 250K. And the rate of hydrogen release for DADB system increases slowly until around 1250K, and then peaks at 2500K, and the whole dehydrogenation process completes at around 3500K. The release of its first and second equivalent hydrogen molecule occurs at around 1500K and 2200K, similar to that of AADB. We also observed that with the anion $[BH_4]^-$, the cleavages of B–N bonds tend to occur.

Figure 2 plots the averaged molecular weight (MW) of boron and nitrogen containing molecules and the total number of B–N bonds versus temperature for the temperature ramp-

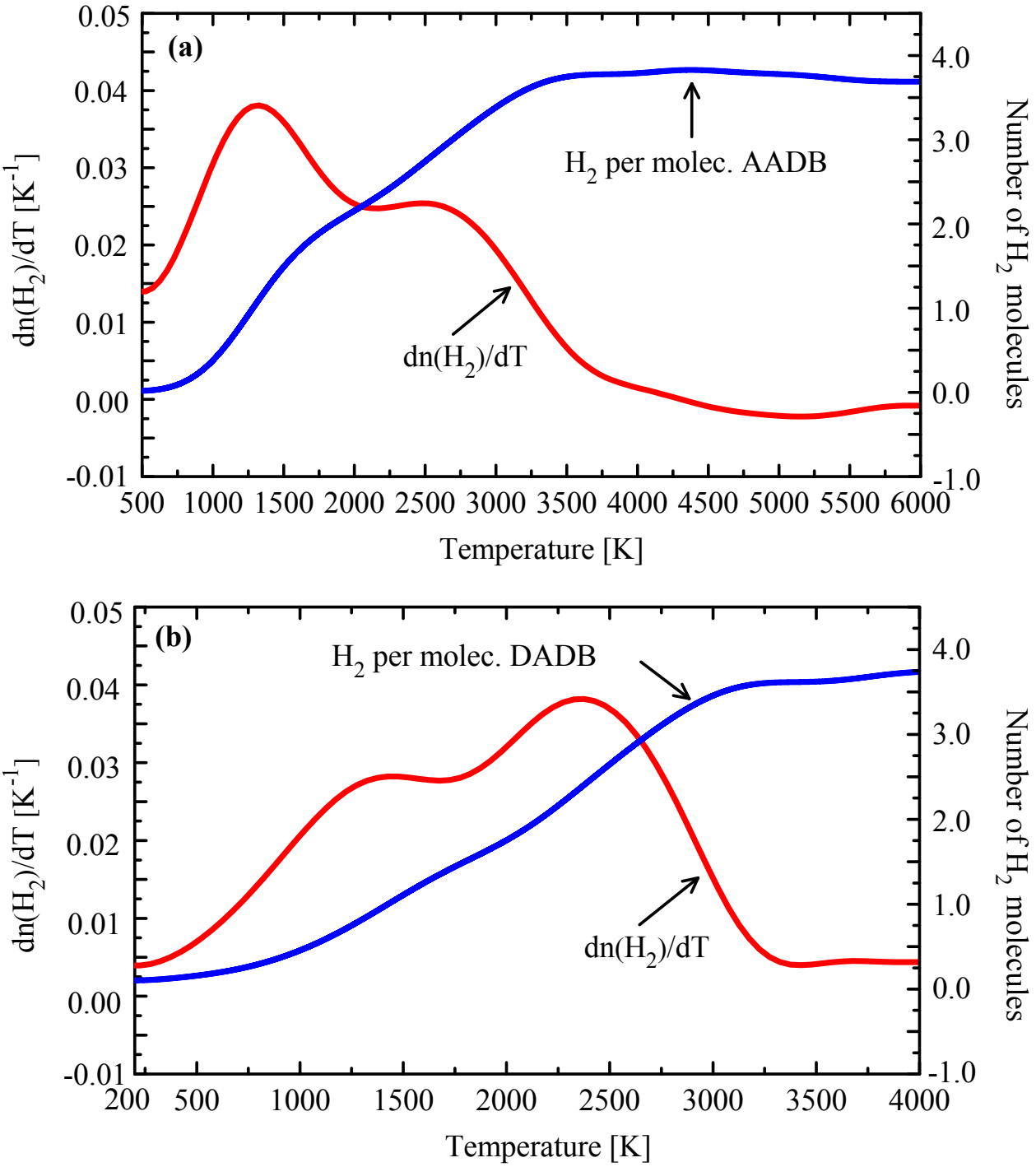

Figure 1: Rate of hydrogen release per change in the reference temperature of the bath for temperature ramping MD simulations of (a) AADB and (b) DADB.

ing simulations of AADB and DADB. In the case of AADB (Figure 2a), initially, after the system was heated to around 1000K, both the averaged MW of boron and nitrogen contain-

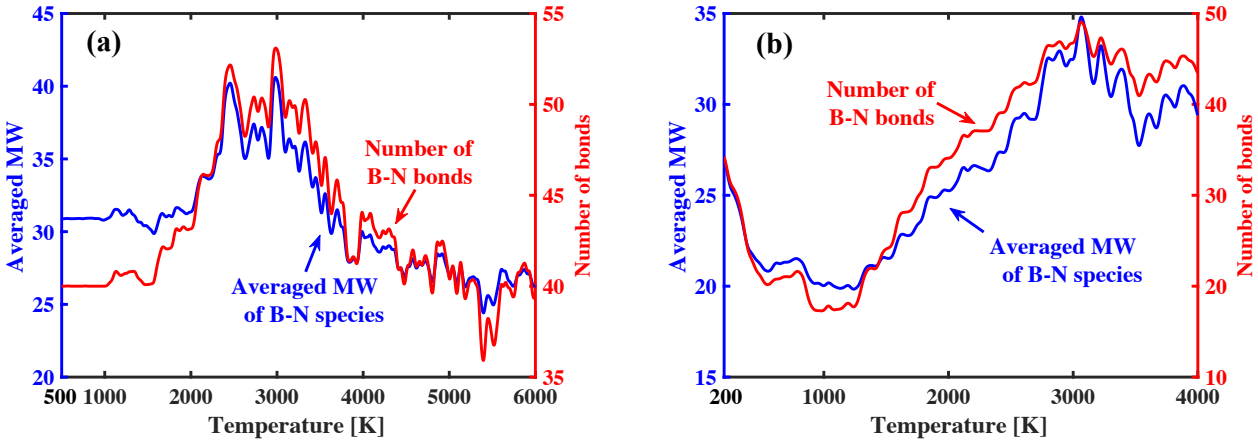

Figure 2: The averaged molecular weight (MW) of the boron and nitrogen containing molecules and the total number of B–N bonds for temperature ramping simulations of (a) AADB and (b) DADB.

ing molecules and the total number of B–N bonds began to increase until 2500K. This process was accompanied with a similar tendency of hydrogen release, as shown in Figure 1a. At the beginning stage of the simulation, after hydrogen was release via the dissociation of hydrogen atoms from B or N, new B–N bonds can be formed, and these formed bonds are relatively stable at lower temperatures. Between 2500K and 3000K, the rate of hydrogen release was observed to decrease (Figure 1a), and the formed big molecules appear to be unstable as we noticed that the cleavages and formations of B–N bonds occur with high frequencies. The averaged MW of these boron and nitrogen containing species and the total number of B–N bonds are also fluctuating heavily. Once the temperature is higher than 3000K, those newly formed B–N bonds are not stable, and begin to break, as the averaged MW of these formed molecules also begins to drop. Such an observation is consistent with the work by Weismiller *et al.* in simulations of AB.[33] They reported that the newly formed boron and nitrogen containing molecules begin to break apart when the temperature is higher than 2500K.

In the case of simulation of DADB (Figure 2b), the observed phenomenon is different from that of AADB. Both the averaged MW of the boron and nitrogen containing molecules and number of B–N bonds begin to drop when the system was heated to around 250K, and this tendency prevailed until around 1000K. This is consistent with the work by Chen

et al., in which they reported that the boron-containing anion $[BH_4]^-$ cannot extend the N−B−N skeleton.[27] The role played by this anion $[BH_4]^-$ in the cleavage of B−N bond will be investigated with DFT calculations, and more details will be provided below. When the temperature of the system reached around 1000K, we can observe the formations of new B–N bonds, as both the averaged MW of the boron and nitrogen containing molecules and the total number of B–N bonds begin to increase. Such a tendency lasts until around 3000K (similar to AADB, Figure 2a). This process was accompanied by hydrogen release (Figure 1b). When the temperature of this system reached between 2500K and 3000K, large fluctuations of both the averaged MW of the boron and nitrogen containing molecules and the total number of B–N bonds were also observed.

Table 2: Summary of observed dehydrogenation pathways for AADB and DADB

AADB	DADB
$NB_2H_8 \longrightarrow NB_2H_7 + H$	$BN_2H_8 \longrightarrow BNH_5 + NH_3$
$NB_2H_8 + NH_4 \longrightarrow NH_3 + NB_2H_7 + H_2$	$BNH_5 + BH_4 \longrightarrow BNH_4 + BH_3 + H_2$
$NB_2H_7 + NB_2H_7 \longrightarrow 2\,NB_2H_6 + H_2$	$BNH_5 \longrightarrow BNH_3 + H_2$
$NB_2H_6 + NB_2H_7 \longrightarrow NB_2H_5 + NB_2H_6 + H_2$	$BNH_3 + BNH_3 \longrightarrow BNH_2 + BNH_2 + H_2$
$NB_2H_7 + H \longrightarrow NB_2H_6 + H_2$	$BN_2H_8 \longrightarrow BN_2H_6 + H_2$
$N_2B_2H_6 + NH_3 \longrightarrow N_3B_2H_9$	$BNH_3 \longrightarrow BNH + H_2$
$N_2B_2H_6 \longrightarrow N_2B_2H_4 + H_2$	$B_2NH_5 + BH_4 \longrightarrow B_2NH_4 + BH_3 + H_2$
$NB_2H_7 \longrightarrow NB_2H_5 + H_2$	$BH_3 + NH_3 \longrightarrow BNH_4 + H_2$
$NB_2H_5 \longrightarrow NB_2H_3 + H_2$	$BNH_4 + BH_4 \longrightarrow BNH_3 + BH_3 + H_2$
$NB_2H_6 \longrightarrow NB_2H_4 + H_2$	$BNH_4 \longrightarrow BNH_2 + H_2$
$NB_2H_6 \longrightarrow NBH_3 + BH_3$	$BN_2H_6 + BH_4 \longrightarrow BN_2H_5 + BH_3 + H_2$
$NBH_3 + NB_2H_5 \longrightarrow NBH_2 + NB_2H_4 + H_2$	$BN_2H_5 + BNH_3 \longrightarrow BN_2H_4 + BNH_2 + H_2$
$NBH_3 + NB_2H_3 \longrightarrow N_2B_3H_4 + H_2$	$BN_2H_5 \longrightarrow BN_2H_3 + H_2$
$NBH_3 + NB_2H_6 \longrightarrow N_2B_3H_7 + H_2$	$BN_2H_3 + BH_3 \longrightarrow B_2N_2H_6$
$N_2B_3H_7 \longrightarrow N_2B_3H_5 + H_2$	$B_2N_2H_6 + H \longrightarrow B_2N_2H_5 + H_2$
$NBH_3 + NB_2H_8 \longrightarrow N_2B_3H_9 + H_2$	$B_2N_2H_6 \longrightarrow B_2N_2H_4 + H_2$
$N_2B_3H_9 \longrightarrow N_2B_3H_7 + H_2$	$B_2N_2H_5 \longrightarrow B_2N_2H_3 + H_2$

The structures of the products can be found in ESI Table S1.

DFT calculations of the dehydrogenation pathways

Based on the findings of our simulations discussed above, DFT calculations of the dehydrogenation pathways for these two molecules were also conducted at the level of M062X/6-

311++G(d,p). From the simulation of AADB, we identified two important dehydrogenation pathways: inter-molecular and intra-molecular. The energy barrier of inter-molecular dehydrogenation (Figure 3a, 17.0 kcal/mol) is much lower than that of intra-molecular dehydrogenation (Figure 3b, 50.8 kcal/mol).

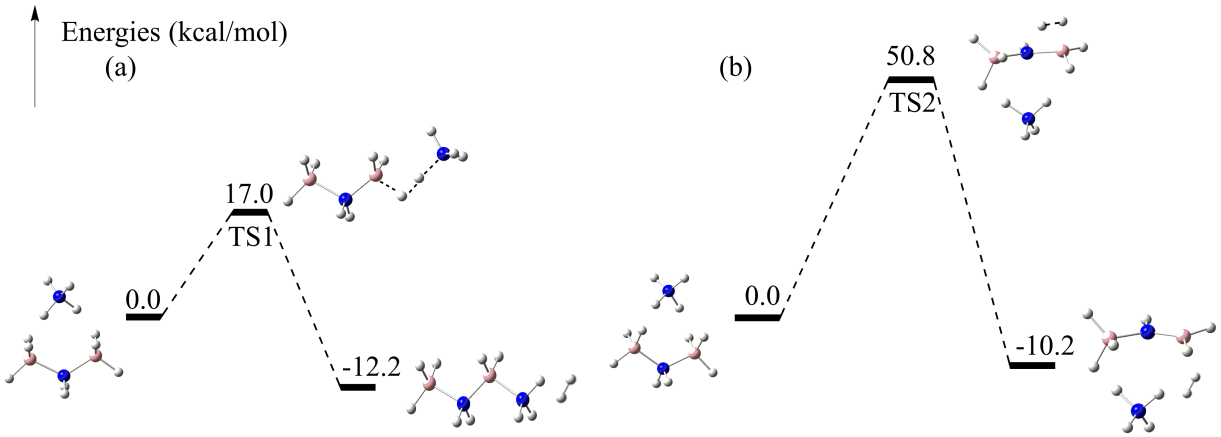

Figure 3: Dehydrogenation pathways for AADB. (a). Inter-molecular dehydrogenation; (b). Intra-molecular dehydrogenation. The relative energies were obtained from M062X/6-311++G(d,p) calculations + ZPE corrections.

From the simulations of DADB, we observed the cleavage of B−N bonds within the cations, with the corresponding hydrogen release. Based on the previous study by Dixon and co-workers on AB,[41] we learned that AB molecules might undergo the cleavage of B–N bond preferentially and give NH_3 and BH_3. This is consistent with our findings from ReaxFF MD simulations of DADB. In Figure 4a, the energy barrier of breaking the B–N bond in DADB molecules were shown. The distributions of the electron density for the states during the cleavage of B–N bond through TS3 were included in ESI Figure S13. It confirmed the cleavage of the B–N bond inside $[NH_3-BH_2-NH_3]^+$ is almost complete at the transition state. The dehydrogenation of DADB (after the cleavage of B−N bonds inside the anions), largely depends on the boron-containing anion $[BH_4]^-$, and the interaction between the intermediate $NH_3-BH_2--H--BH_3$ and NH_3. The same interaction was revealed by the metadynamics simulations of AB by Rizzi *et al.*[23] We infer that the hydrogen release via this dihydrogen interaction between $B-H^{\delta-}$ and $N-H^{\delta+}$ can be further facilitated, as noted

by Chen *et al.*[27]

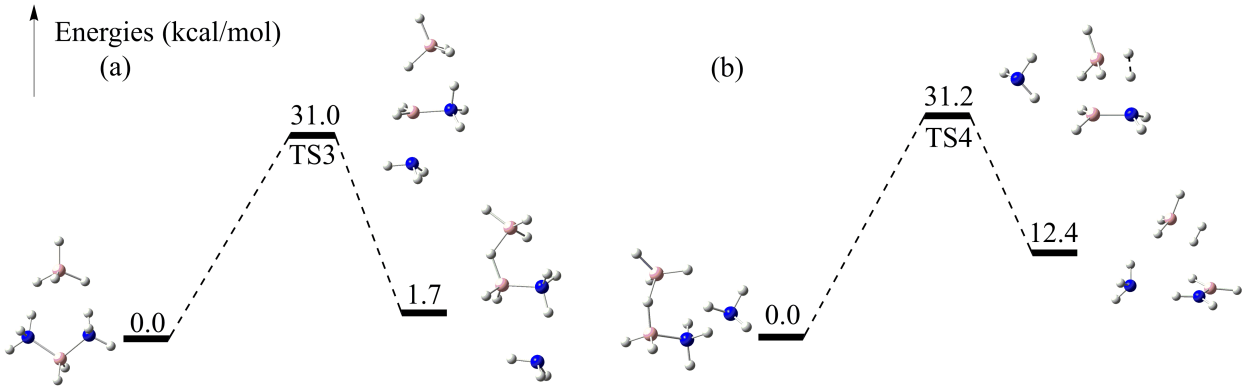

Figure 4: Dehydrogenation pathways for DADB. (a). The breaking of B–N bond; (b).Intramolecular dehydrogenation after the cleavage of B–N bond. The relative energies were obtained from M062X/6-311++G(d,p) calculations + ZPE corrections.

We would like to note that our current work focused only on these two potential dehydrogenation pathways. The DFT calculations were mainly applied to verify the observations from MD simulations with ReaxFF. However, beyond these investigated dehydrogenation pathways, there may exist some other transition states with lower energies, which require future investigations to reveal the exact routes connecting the various intermediate states.

Constant temperature MD simulations of AADB and DADB

In addition to the temperature ramping simulations, we also studied the dehydrogenation process at constant temperature conditions. Figure 5 plots the number of released hydrogen molecules as a function of simulation time for these two molecules at constant temperature simulations (1500K, 2000K, 2500K and 3000K). These temperatures were chosen for these two systems because they correspond to where the largest amount of the formation and dissociation of B−N bonds were observed in the temperature ramping simulations (Figure 1). We can see that for both the molecules, the maximum amount of hydrogen release increases with temperature. Moreover, at 1500K and 2000K, we found that the dehydrogenation of AADB is more complete than that of DADB.

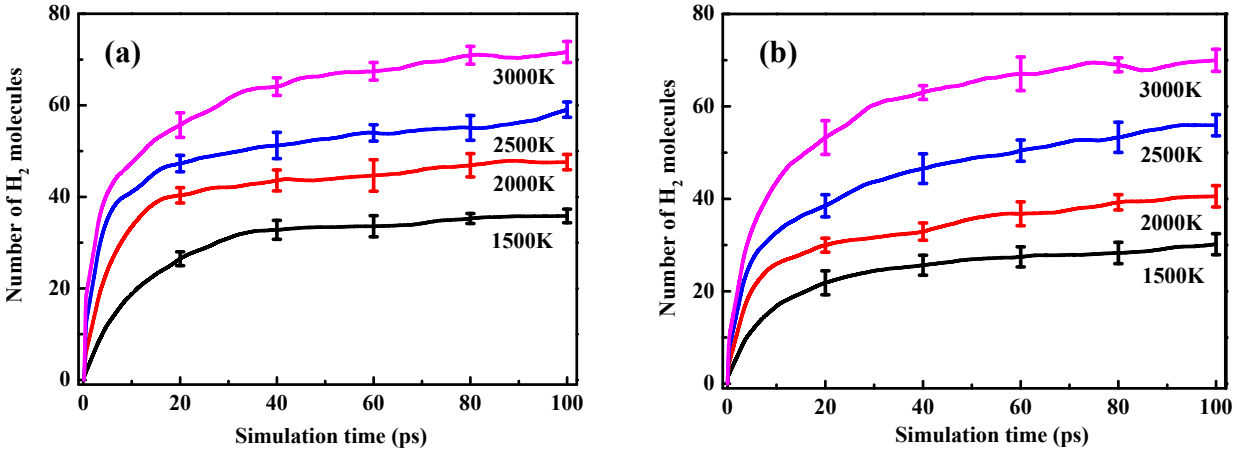

Figure 5: Hydrogen release versus time for the simulations of (a) AADB and (b) DADB at various temperatures. For each simulation, five independent simulations were carried out for averaging, and the root-mean-square deviations are shown.

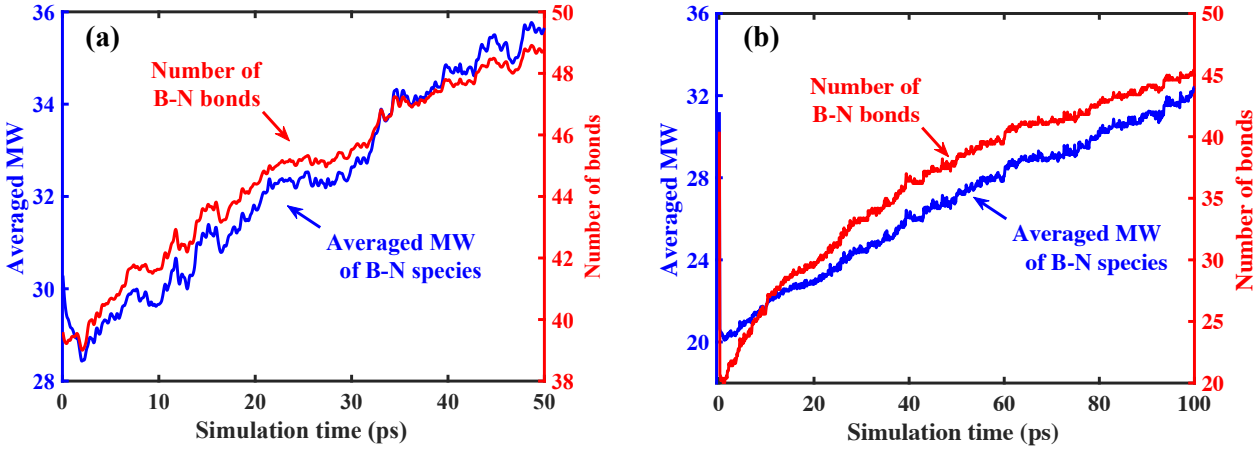

Figure 6: The averaged molecular weight (MW) of boron and nitrogen containing molecules and the total number of B–N bonds versus simulation time for constant temperature simulations (2500K) of (a) AADB and (b) DADB. For each simulation, five independent simulations were carried out for averaging.

Figure 6 plots the averaged MW of the boron and nitrogen containing molecules and the total number of B–N bonds as the function of simulation time for AADB and DADB at 2500K. For AADB, consistent with the findings described above, its dehydrogenation is correlated with the formations of B–N bonds. In the case of DADB, the decomposition of this molecule can occur at a lower temperature, therefore, both the averaged MW of the boron and nitrogen containing molecules and the total number of B–N bonds firstly dropped to a lower value. However, the reformations of new B–N bonds were also observed in the

later simulations, and the averaged MW of the boron and nitrogen containing molecules tend to increase following the tendency of the total number of B–N bonds.

Conclusions

Ammonium aminodiboranate (AADB) and diammoniate of diborane (DADB) are two important isomers of ammonia borane (AB). In the current work, MD simulations with ReaxFF were applied to investigate their dehydrogenation pathways. From the temperature ramping simulations, the correlation between temperature and the amount of their hydrogen release were revealed. In the case of AADB, at lower temperatures, the hydrogen release was mainly realised via inter-molecular dehydrogenations, and the rate of hydrogen release was shown to peak at around 1200 K. As the temperature increases, its hydrogen release tends to occur via intra-molecular dehydrogenation. This is consistent with the barriers of these two dehydrogenation pathways based on the DFT calculations. For DADB, the temperature ramping simulations showed that even at low temperature (around 250K), with the existence of a boron-containing anion ($[BH_4]^-$), the cation ($[NH_3-BH_2-NH_3]^+$) will first decompose with the cleavage of B–N bonds; moreover, such an anion can also facilitate the dihydrogen interactions between $B-H^{\delta-}$ and $N-H^{\delta+}$, which leads to further hydrogen release. Through the DFT calculations, the corresponding dehydrogenation pathway for DADB was also verified. The detailed analyses of the potential reaction pathways could provide insight for future studies based on advanced sampling techniques with more accurate models. It is worth noting that, our current temperature ramping simulations are a first attempt to understand the dehydrogenation pathways of AADB and DADB. There are a few aspects worth further investigations. First, our simulated systems do not represent the realistic experimental conditions where the dehydrogenation often initiated from a solid-state or in a solution. This can be considered as in the study by Rizzi *et al.*[23] Second, a specific heating rate was chosen following the study of Weismiller *et al.*[33] Different heating rates may impact the rates of

their hydrogen release quantitatively. Last, the role of solvents remains to be explored in future studies. Nevertheless, based on the current study, we can conclude that for AADB and DADB, the composition of their cations and anions can impact their hydrogen release; and ReaxFF was shown to be a computationally attractive tool to carry out the initial investigations of their dehydrogenation pathways.

Acknowledgement

We wish to acknowledge the Australian Government for an Australian International Postgraduate Award scholarship for P.G. This research was in part supported under the Australian Research Council's Discovery Projects funding scheme (project number DP170101773). We wish to acknowledge that this research was undertaken with the assistance of resources provided at the NCI National Facility systems at the Australian National University through the National Computational Merit Allocation Scheme supported by the Australian Government (Project id: v15).

Supporting Information Available

Related statistic analysis can be founded in Supporting Information.

This material is available free of charge via the Internet at `http://pubs.acs.org/`.

References

(1) Züttel, A. Hydrogen storage methods. *Naturwissenschaften* **2004**, *91*, 157–172.

(2) Züttel, A. Materials for hydrogen storage. *Materials Today* **2003**, *6*, 24–33.

(3) Huang, Z.; Autrey, T. Boronnitrogenhydrogen (BNH) compounds: recent developments

in hydrogen storage, applications in hydrogenation and catalysis, and new syntheses. *Energy Environ. Sci.* **2012**, *5*, 9257–9268.

(4) Sakintuna, B.; Lamari-Darkrim, F.; Hirscher, M. Metal hydride materials for solid hydrogen storage: A review. *International Journal of Hydrogen Energy* **2007**, *32*, 1121–1140.

(5) Bogdanović, B.; Schwickardi, M. Ti-doped alkali metal aluminium hydrides as potential novel reversible hydrogen storage materials1Invited paper presented at the International Symposium on Metal−Hydrogen Systems. *Journal of Alloys and Compounds* **1997**, *253-254*, 1–9.

(6) Graetz, J. New approaches to hydrogen storage. *Chem. Soc. Rev.* **2009**, *38*, 73–82.

(7) Züttel, A.; Wenger, P.; Rentsch, S.; Sudan, P.; Mauron, P.; Emmenegger, C. LiBH4 a new hydrogen storage material. *Journal of Power Sources* **2003**, *118*, 1–7.

(8) Teichmann, D.; Stark, K.; Müller, K.; Zöttl, G.; Wasserscheid, P.; Arlt, W. Energy storage in residential and commercial buildings via Liquid Organic Hydrogen Carriers (LOHC). *Energy Environ. Sci.* **2012**, *5*, 9044–9054.

(9) Campbell, P. G.; Zakharov, L. N.; Grant, D. J.; Dixon, D. A.; Liu, S.-Y. Hydrogen Storage by Boron-Nitrogen Heterocycles: A Simple Route for Spent Fuel Regeneration. *Journal of the American Chemical Society* **2010**, *132*, 3289–3291.

(10) Luo, W.; Campbell, P. G.; Zakharov, L. N.; Liu, S.-Y. A Single-Component Liquid-Phase Hydrogen Storage Material. *Journal of the American Chemical Society* **2011**, *133*, 19326–19329.

(11) Luo, W.; Zakharov, L. N.; Liu, S.-Y. 1,2-BN Cyclohexane: Synthesis, Structure, Dynamics, and Reactivity. *Journal of the American Chemical Society* **2011**, *133*, 13006–13009.

(12) Chen, G.; Zakharov, L. N.; Bowden, M. E.; Karkamkar, A. J.; Whittemore, S. M.; Garner, E. B.; Mikulas, T. C.; Dixon, D. A.; Autrey, T.; Liu, S.-Y. Bis-BN Cyclohexane: A Remarkably Kinetically Stable Chemical Hydrogen Storage Material. *Journal of the American Chemical Society* **2015**, *137*, 134–137.

(13) Marder, T. Will We Soon Be Fueling our Automobiles with AmmoniaBorane? *Angewandte Chemie International Edition* **2007**, *46*, 8116–8118.

(14) Stephens, F. H.; Pons, V.; Tom Baker, R. Ammoniaborane: the hydrogen source par excellence? *Dalton Trans.* **2007**, 2613–2626.

(15) Demirci, U. B. Ammonia borane, a material with exceptional properties for chemical hydrogen storage. *International Journal of Hydrogen Energy* **2017**, *42*, 9978–10013.

(16) Staubitz, A.; Robertson, A. P. M.; Manners, I. Ammonia-Borane and Related Compounds as Dihydrogen Sources. *Chemical Reviews* **2010**, *110*, 4079–4124.

(17) Xu, Q.; Chandra, M. Catalytic activities of non-noble metals for hydrogen generation from aqueous ammoniaborane at room temperature. *Journal of Power Sources* **2006**, *163*, 364–370.

(18) Chandra, M.; Xu, Q. A high-performance hydrogen generation system: Transition metal-catalyzed dissociation and hydrolysis of ammoniaborane. *Journal of Power Sources* **2006**, *156*, 190–194.

(19) Chandra, M.; Xu, Q. Room temperature hydrogen generation from aqueous ammoniaborane using noble metal nano-clusters as highly active catalysts. *Journal of Power Sources* **2007**, *168*, 135–142.

(20) Daly, S. R.; Bellott, B. J.; Kim, D. Y.; Girolami, G. S. Synthesis of the Long-Sought Unsubstituted Aminodiboranate Na(H_3B-NH_2-BH_3) and Its N-Alkyl Analogs. *Journal of the American Chemical Society* **2010**, *132*, 7254–7255.

(21) Ewing, W. C.; Marchione, A.; Himmelberger, D. W.; Carroll, P. J.; Sneddon, L. G. Syntheses and Structural Characterizations of Anionic Borane-Capped Ammonia Borane Oligomers: Evidence for Ammonia Borane H_2 Release via a Base-Promoted Anionic Dehydropolymerization Mechanism. *Journal of the American Chemical Society* **2011**, *133*, 17093–17099.

(22) Chen, W.; Yu, H.; Wu, G.; He, T.; Li, Z.; Guo, Z.; Liu, H.; Huang, Z.; Chen, P. Ammonium Aminodiboranate: A Long-Sought Isomer of Diammoniate of Diborane and Ammonia Borane Dimer. *Chemistry A European Journal* **2016**, *22*, 7727–7729.

(23) Rizzi, V.; Polino, D.; Sicilia, E.; Russo, N.; Parrinello, M. The Onset of Dehydrogenation in Solid Ammonia Borane: An Ab Initio Metadynamics Study. *Angewandte Chemie* **2019**, *131*, 4016–4020.

(24) Nguyen, V. S.; Matus, M. H.; Grant, D. J.; Nguyen, M. T.; Dixon, D. A. Computational Study of the Release of H_2 from Ammonia Borane Dimer $(BH_3NH_3)_2$ and Its Ion Pair Isomers. *The Journal of Physical Chemistry A* **2007**, *111*, 8844–8856.

(25) Chen, X.; Bao, X.; Zhao, J.-C.; Shore, S. G. Experimental and Computational Study of the Formation Mechanism of the Diammoniate of Diborane: The Role of Dihydrogen Bonds. *Journal of the American Chemical Society* **2011**, *133*, 14172–14175.

(26) Autrey, T.; Bowden, M.; Karkamkar, A. Control of hydrogen release and uptake in amine borane molecular complexes: thermodynamics of ammonia borane, ammonium borohydride, and the diammoniate of diborane. *Faraday Discuss.* **2011**, *151*, 157–169.

(27) Chen, X.-M.; Liu, S.-C.; Xu, C.-Q.; Jing, Y.; Wei, D.; Li, J.; Chen, X. Unravelling a general mechanism of converting ionic B/N complexes into neutral B/N analogues of alkanes: $H^{\delta+}\cdots H^{\delta-}$ dihydrogen bonding assisted dehydrogenation. *Chemical Communications* **2019**, *55*, 12239–12242.

(28) Grant, D. J.; Matus, M. H.; Anderson, K. D.; Camaioni, D. M.; Neufeldt, S. R.; Lane, C. F.; Dixon, D. A. Thermochemistry for the Dehydrogenation of Methyl-Substituted Ammonia Borane Compounds. *The Journal of Physical Chemistry A* **2009**, *113*, 6121–6132.

(29) van Duin, A. C. T.; Dasgupta, S.; Lorant, F.; Goddard, W. A. ReaxFF: A Reactive Force Field for Hydrocarbons. *The Journal of Physical Chemistry A* **2001**, *105*, 9396–9409.

(30) Aktulga, H.; Pandit, S.; van Duin, A.; Grama, A. Reactive Molecular Dynamics: Numerical Methods and Algorithmic Techniques. *SIAM Journal on Scientific Computing* **2012**, *34*, C1–C23.

(31) Kim, S.-Y.; Kumar, N.; Persson, P.; Sofo, J.; van Duin, A. C. T.; Kubicki, J. D. Development of a ReaxFF Reactive Force Field for Titanium Dioxide/Water Systems. *Langmuir* **2013**, *29*, 7838–7846.

(32) Bedrov, D.; Smith, G. D.; van Duin, A. C. T. Reactions of Singly-Reduced Ethylene Carbonate in Lithium Battery Electrolytes: A Molecular Dynamics Simulation Study Using the ReaxFF. *The Journal of Physical Chemistry A* **2012**, *116*, 2978–2985.

(33) Weismiller, M. R.; van Duin, A. C. T.; Lee, J.; Yetter, R. A. ReaxFF Reactive Force Field Development and Applications for Molecular Dynamics Simulations of Ammonia Borane Dehydrogenation and Combustion. *The Journal of Physical Chemistry A* **2010**, *114*, 5485–5492.

(34) Pai, S. J.; Yeo, B. C.; Han, S. S. Development of the ReaxFFCBN reactive force field for the improved design of liquid CBN hydrogen storage materials. *Phys. Chem. Chem. Phys.* **2016**, *18*, 1818–1827.

(35) Han, S. S.; Kang, J. K.; Lee, H. M.; van Duin, A. C. T.; Goddard, W. A. The theoretical study on interaction of hydrogen with single-walled boron nitride nanotubes. I. The

reactive force field ReaxFFHBN development. *The Journal of Chemical Physics* **2005**, *123*, 114703.

(36) Han, S. S.; Kim, H. S.; Han, K. S.; Lee, J. Y.; Lee, H. M.; Kang, J. K.; Woo, S. I.; van Duin, A. C. T.; Goddard, W. A. Nanopores of carbon nanotubes as practical hydrogen storage media. *Applied Physics Letters* **2005**, *87*, 213113.

(37) Cheung, S.; Deng, W.-Q.; van Duin, A. C. T.; Goddard, W. A. ReaxFFMgH Reactive Force Field for Magnesium Hydride Systems. *The Journal of Physical Chemistry A* **2005**, *109*, 851–859.

(38) Plimpton, S. Fast Parallel Algorithms for Short-Range Molecular Dynamics. *Journal of Computational Physics* **1995**, *117*, 1–19.

(39) Luo, W.; Campbell, P. G.; Zakharov, L. N.; Liu, S.-Y. A Single-Component Liquid-Phase Hydrogen Storage Material. *Journal of the American Chemical Society* **2011**, *133*, 19326–19329.

(40) Frisch, M. J.; Trucks, G. W.; Schlegel, H. B.; Scuseria, G. E.; Robb, M. A.; Cheeseman, J. R.; Scalmani, G.; Barone, V.; Mennucci, B.; Petersson, G. A. et al. Gaussian 09 Revision E.01. Gaussian Inc. Wallingford CT 2009.

(41) Nguyen, M. T.; Nguyen, V. S.; Matus, M. H.; Gopakumar, G.; Dixon, D. A. Molecular Mechanism for H_2 Release from BH_3NH_3, Including the Catalytic Role of the Lewis Acid BH_3. *The Journal of Physical Chemistry A* **2007**, *111*, 679–690.

Graphical TOC Entry